



# IoT-Based Non-Invasive RBI Index Detection using Electrocardiogram Photoplethysmogram Signals with Firebase Cloud Integration and Real-Time Health Alerts

Gaayathry K<sup>1</sup>, Adithya G<sup>2\*</sup>, Shasvanth J<sup>3</sup>, Vethesnan P J<sup>4</sup>

<sup>1</sup>Associate Professor, Department of ICE, Saranathan College of Engineering, Tiruchirappalli, Tamil Nadu, India.

<sup>2</sup>Student, Department of ICE, Saranathan College of Engineering, Tiruchirappalli, Tamil Nadu, India.

<sup>3</sup>Student, Department of ICE, Saranathan College of Engineering, Tiruchirappalli, Tamil Nadu, India.

<sup>4</sup>Student, Department of ICE, Saranathan College of Engineering, Tiruchirappalli, Tamil Nadu, India.

Corresponding author(s):

DoI: <https://doi.org/10.5281/zenodo.19338322>

Adithya G, Student, Department of ICE, Saranathan College of Engineering, Tiruchirappalli, Tamil Nadu, India.

Email: [adithya8705@gmail.com](mailto:adithya8705@gmail.com)

Citation:

Gaayathry K, Adithya G\*, Shasvanth J, Vethesnan P J (2026). IoT-Based Non-Invasive RBI Index Detection using Electrocardiogram(ECG) Photoplethysmogram(PPG) Signals with Firebase Cloud Integration and Real-Time Health Alerts. International Journal of Multidisciplinary Research Transactions, 8(4), 21–45. <https://doi.org/10.5281/zenodo.19338322>

This article is an open access article distributed under the terms and conditions of the Creative Commons Attribution CC BY) license (<https://creativecommons.org/licenses/by/4.0/>).

Accepted: 24 March 2026

Available online: 30 March 2026

## Abstract

Peripheral artery disease is a chronic circulatory disorder that is manifested by narrowing or obstruction of peripheral arteries, mainly lower limbs. Early diagnosis is crucial to avoid severe complications: critical limb ischemia, myocardial infarction, and stroke. However, these diagnostic methods require clinical setups and trained professionals for their operation, limiting accessibility during early or continuous screening. This paper proposes the design and prototype implementation of a wearable device for early PAD detection based on multi-sensor data fusion. The system is integrated with Electrocardiogram (ECG), Photoplethysmogram (PPG), and bioimpedance sensors to monitor vascular health continuously. With this setup, Pulse transit time (PTT) and Pulse wave velocity (PWV) are computed as surrogate markers of arterial stiffness, and simultaneous bioimpedance data complement vascular tone information. The microcontroller-based system (ESP32) performs real-time data acquisition,

---

pre-processing, and wireless transmission via Bluetooth Low Energy (BLE) to a mobile application for visualization. Preliminary tests on healthy volunteers confirm successful synchronization of ECG and PPG signals, demonstrating the feasibility of non-invasive vascular monitoring. Future work includes the machine-learning-based PAD stage classification and clinical validation. A cost-effective, portable, continuous monitoring solution is provided by the proposed device, which can be used for early diagnosis and management of PAD.

**Keywords:** Peripheral Artery Disease, Wearable Sensor, Electrocardiogram, Photoplethysmogram, Bioimpedance, Pulse Transit Time, Pulse Wave Velocity, Data Fusion.

---

## 1. Introduction

PAD is a progressive vascular disorder due to the accumulation of atherosclerotic plaque, leading to stenosis or occlusion of the arteries in the extremities. The diminished blood flow results in pain, fatigability, or trophic ulcers and may lead to tissue necrosis and amputation of the extremity in advanced disease. The WHO estimates that more than 200 million people worldwide suffer from PAD, most of whom remain asymptomatic and undiagnosed in early stages. PAD is strongly linked to diabetes, hypertension, and smoking; it also acts as an early marker of cardiovascular events and mortality.

While traditional diagnostic techniques, such as the ankle-brachial index, are very reliable, they do require Doppler ultrasound machinery and professionals who know how to use such equipment. These tests are point-in-time in nature and cannot represent dynamic vascular changes. The clinical and technologically increasing demand is, hence, toward the development of noninvasive, continuous, and accessible diagnostic systems that would be able to detect hemodynamic changes indicative of PAD.

Recent developments in both wearable technology and physiological signal processing have enabled the continuous monitoring of cardiovascular activity outside clinical settings. ECG and PPG sensors may provide an estimate of PTT and PWV, surrogate markers of arterial stiffness and blood vessel compliance, respectively. At the same time, bioimpedance sensing allows the determination of tissue perfusion and vascular tone, providing complementary information on peripheral circulation.

This paper proposes a wearable multi-sensor device that integrates these three modalities-ECG, PPG, and bioimpedance-on a compact platform for real-time monitoring. Such an

integration can enable early detection of PAD by data fusion, signal synchronization, and feature extraction, thereby bridging the gap between hospital-based diagnostics and preventive home-based healthcare.

## **2. Literature Review**

This has made PAD an important area of growth interest, as many systemic cardiovascular complications are strongly related to PAD. Traditional diagnostic modalities include ABI and Doppler ultrasound that remain the clinical standard; however, these are limited by the need for skilled operators and static, point-in-time measurements. Thus, Wearable sensing for early detection and continuous vascular monitoring of PAD has gained rapid attention in current research.

### **2.1. Evolution of wearable vascular monitoring**

The initial contribution of Allen (2007) has positioned the photoplethysmogram as a useful non-invasive tool to measure characteristic properties of an arterial pulse. Subsequent to this, PPG has been widely applied in wrist-worn devices and mobile health systems. Zheng et al., 2018 showed that pulse transit time, obtained from synchronized ECG and PPG signals, can act as a surrogate for arterial stiffness and blood pressure. Their results shed light on further studies that combined multimodal physiological sensing for cardiovascular screening.

The review by Pantelopoulos and Bourbakis (2010) on wearable health-monitoring systems emphasized the need for multi-sensor fusion as a way to improve diagnostic reliability. Although single sensors have shown great advancement, how multiple physiological parameters-especially those sensitive to motion, skin tone, and temperature-can be combined is an active research topic.

### **2.2. Multimodal sensing approaches**

Recent studies have concentrated on combining complementary biosignals to derive a holistic vascular condition. Smith et al. (2021) have proposed a wearable bioimpedance device that measures vascular resistance and peripheral tone but does not provide cardiac timing information, which is usually much sought after for accurate hemodynamic analysis. Metshein et al. (2023) furthered this by co-measuring PPG and bioimpedance signals from the same and different sites on the limbs to quantify peripheral arterial properties. Such multiple-sensor

designs show high sensitivity to arterial occlusion compared with single-sensor approaches. In parallel, Hong and Coté (2024) developed a tetherless bioimpedance system that could detect morphologic vascular impedance changes corresponding to simulated PAD progression. Findings from their investigation supported the capability of impedance plethysmography to execute continuous vascular monitoring under free-living conditions. Similarly, Wu et al. (2024) reviewed advances in interstitial-fluid-based wearable biosensors, highlighting miniaturization and low-power operation, one of many key features necessary for the 24-hour monitoring of hemodynamic trends.

### **2.3. Artificial Intelligence and data fusion in PAD diagnosis**

As sensing hardware matured, the focus of PAD research has shifted toward intelligent data processing. Machine learning techniques are increasingly employed to classify the severity of PAD and predict vascular events. Zhang et al., 2023, proved that gait biomechanics coupled with neural network models can distinguish between PAD patients and healthy individuals with a high degree of accuracy. In wearable systems, data-driven algorithms were suggested by both Metshein et al., 2023, and Hong & Coté, 2024, for the correction of motion artifacts and ambient noise, which greatly enhances the measurement fidelity.

The fusion of ECG, PPG, and bioimpedance signals will therefore provide richer temporal and amplitude-based features for AI models. Tay et al. (2022) have shown hybrid models that integrate temporal PTT features with phase bioimpedance data to yield up to 25% improved arterial stiffness prediction over more traditional regression methods. Rahman et al. (2021) applied a support vector machine to classify the severity of PAD using multisite PPG waveforms, further illustrating the potential of machine learning for automated screening.

### **2.4. Recent Advances in Smart Wearables**

Over the last five years, commercial and research prototypes have targeted vascular health beyond simple heart-rate monitoring. Li et al. (2022) designed a flexible wrist-ankle PPG system for peripheral circulation assessment, achieving strong correlation with Doppler ultrasound readings. Recently, Park et al. (2023) developed a soft bioimpedance patch integrated with Bluetooth communication for continuous arterial stiffness monitoring. A 2024 narrative review on smart wearables for non-coronary vascular disease has emphasized the need for multimodal, longitudinal datasets to train predictive PAD algorithms.

Chowdhury et al. (2023) have studied the impact of temperature and ambient light on PPG sensor accuracy and proposed adaptive filtering methods suitable for wearable PAD detection systems. Their results favor incorporating environmental compensation along with motion sensors such as accelerometers to make them more robust.

## 2.5 Research gaps and motivation

Despite these, there are gaps in attaining reliable, real-time PAD detection outside the clinic.

Most of the currently used systems:

1. Monitor a single physiological signal-usually PPG.
2. Lack of synchronization between central (ECG) and peripheral (PPG/bioimpedance) measurements.
3. Are evaluated mainly in healthy volunteers, with very limited clinical validation in established PAD populations.

Addressing these gaps, this work proposes a tri-modal wearable device that integrates ECG, PPG, and bioimpedance sensors on a unified hardware platform. While performing on-board signal fusion and wireless data transmission, the system allows for real-time computation of pulse transit time and pulse wave velocity, two key indicators of arterial stiffness and peripheral perfusion. This integration is expected to enhance diagnostic reliability and foster the early detection of PAD through continuous, non-invasive monitoring.

## 3. Materials and Methods

### 3.1. System Overview

This system was designed as a wearable, non-invasive device that could be used to acquire several physiological signals simultaneously and estimate arterial stiffness while allowing for the early detection of Peripheral Artery Disease. The core hardware is a microcontroller, selected because it possesses a dual-core processing capability, integrated Bluetooth Low Energy BLE module for ease of use in communication, and low power consumption. The architecture integrates three main sensing subsystems: Electrocardiogram, Photoplethysmogram, and Bioimpedance, which complement the information about vascular and cardiac dynamics. Figure 1 presents the overall architecture of the system, which includes the following parts in order: (1) sensor interfaces, (2) signal conditioning and filtering blocks, (3) analog-to-digital conversion, (4) processing using a microcontroller, and finally, (5) wireless communication and visualization through a mobile or desktop application. The full

system will be a closed-loop acquisition and analysis platform, capable of real-time signal fusion, feature extraction, and data logging for offline analysis.

### 3.1.1. System Block Diagram

Figure 1 presents the overall architecture of the proposed wearable PAD detection system. It shows how ECG, PPG, and bioimpedance sensors are connected through the ESP32 microcontroller along with signal conditioning stages, Bluetooth transmission, and the mobile application interface.

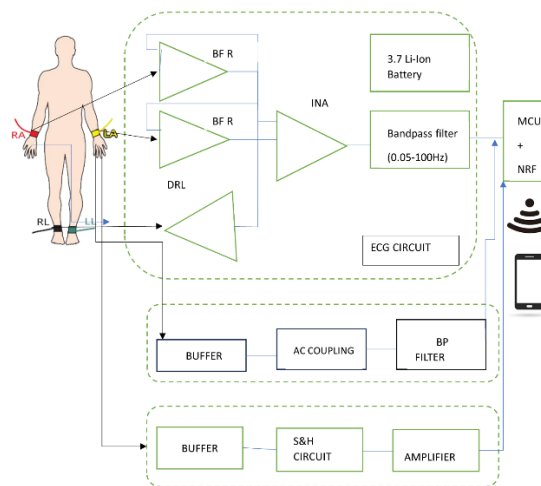


**Figure.1. System Block Diagram**

Figure 1 illustrates the entire pipeline of signal acquisition and processing, starting from physiological signal detection to wireless data transmission and visualization. The proposed system is designed to work in real time for continuous monitoring and computation of hemodynamic parameters such as PTT and PWV.

## 3.2. Sensor Subsystems

### 3.2.1. ECG Module

The ECG subsystem is used to capture cardiac electrical activity by utilizing the AD8232 analog front-end, which offers differential amplification and noise suppression. Three dry electrodes are placed in a modified Lead-II configuration: one at the right wrist, one at the left wrist, and one reference on the lower torso. The AD8232 output is filtered from 0.5-40 Hz in order to eliminate baseline drift and power-line interference. The ECG provides the cardiac timing reference needed to calculate PTT. The peaks of the detected R-wave represent the

electrical onset of ventricular depolarization, corresponding to the start of blood ejection into the arterial system.

### 3.2.2. PPG Module

The MAX30102 optical sensor is used in the PPG subsystem, which comprises infrared (IR) and red LEDs and a photodiode. The IR wavelength is usually utilized for arterial pulse detection, while the red wavelength enables the measurement of peripheral oxygen saturation (SpO<sub>2</sub>). PPG sensors are located in two peripheral positions, one at the wrist and one at the ankle. This setup allows for the measurement of both proximal (central) and distal (peripheral) pulse waves.

The analog PPG signal is digitized at 400 Hz and passed through a second-order Butterworth bandpass filter of 0.3-8 Hz to isolate cardiac pulsations. The first-derivative zero-crossing algorithm is used to perform peak or foot detection, enabling the derivation of temporal markers for PTT computation relative to ECG R-peaks.

### 3.2.3. Bioimpedance Module

The BIOZ subsystem measures the vascular tone and perfusion of tissue by applying a small-alternating current (typically 100  $\mu$ A RMS at 50 kHz) through surface electrodes and measuring the resulting voltage drop. A four-electrode (tetrapolar) configuration minimizes electrode-skin interface impedance. The system makes use of an AD5933 impedance converter IC, which performs excitation and signal demodulation followed by conversion to magnitude and phase data. The magnitude of impedance measured is dependent upon variations in the volume within the arteries that acts as a surrogate measure of peripheral vascular resistance.

## 3.3. Signal Acquisition and Synchronization

Synchronous data acquisition among the ECG, PPG, and BIOZ channels is necessary for accurate feature extraction. Program configuration of the internal timers in the microcontroller generated simultaneous sampling interrupts for each analog input channel. The ECG was sampled at 1 kHz, and PPG and BIOZ signals were sampled at 400 Hz. Before transmission via BLE, all data streams were buffered with synchronized timestamps. The processing of the signals was done in real time using a lightweight filtering and event-detection algorithm implemented in embedded C. This kept latency and power consumption minimal. Synchronization validation was carried out by generating artificial trigger pulses aligned with

ECG R-waves. The resultant PPG waveform timing demonstrated inter-channel drift of less than 2 ms over 5 min recordings, adequate for reliable PTT estimation.

### 3.4. Signal Processing Pipeline

#### 3.4.1. Filtering and Preprocessing

All recorded signals were digitally filtered to suppress noise and motion artifacts. The ECG channel was bandpass-filtered with a Butterworth filter at 0.5 to 40 Hz. This eliminates baseline wander and high-frequency noise. The PPG signal was further bandpass-filtered at 0.3 to 8 Hz and processed by adaptive motion compensation based on accelerometer feedback. Bioimpedance data were low-pass filtered (cutoff 5 Hz).

#### 3.4.2. Feature Extraction

Then, the following features were extracted after preprocessing:

R peak timing from ECG using the Pan–Tompkins algorithm, which combines slope, amplitude and width thresholds.

PPG foot point using the derivative-based zero-crossing detection.

PTT (Pulse Transit Time) computed as:

$$PTT = t_{(PPG\_foot)} - t_{(ECG\_R)}$$

We can compute the PWV from the known inter-sensor distance (D) and measured PTT:

$$PWV = D / PTT$$

BIOZ amplitude and phase to quantify changes in tissue impedance correlated with blood flow.

#### 3.4.3. Data fusion and feature correlation

Feature-level fusion was employed for combining temporal and amplitude information; PTT and PWV represent the central–peripheral hemodynamic response, while bioimpedance magnitude conveys local vascular tone. The fused features were statistically processed to estimate arterial stiffness indices as well as potential PAD indicators.

Vascular elasticity is inferred from the correlation between PWV and bioimpedance amplitude. The change in PTTs from baseline conditions will be indicative of arterial constriction. These combined parameters will then be used as input features for the machine learning-based classification models (Random Forest, SVM, etc.) in future work.

### 3.5. Hardware Integration and Power Management

The entire system was assembled on a custom-designed four-layer Printed Circuit Board (PCB). The microcontroller, sensor modules, and BLE antenna have been integrated into it to minimize trace lengths and electromagnetic interference. The device was powered by a 3.7 V, 500 mAh lithium-ion battery that provides up to 8 hours of continuous operation. Power was regulated using an LDO voltage regulator, while charging was possible by a TP4056 controller. All electrodes were of type silver/silver-chloride Ag/AgCl with medical-grade adhesive backing for safety and comfort. Total device weight was less than 60 grams, suitable for mounting on either the wrist or ankle.

### 3.6. Wireless Data Transmission and Mobile Interface

The microcontroller transmitted acquired data packets via Bluetooth Low Energy (BLE) using the Generic Attribute Profile (GATT) protocol. Each packet consisted of timestamped ECG, PPG, and bioimpedance samples. A custom Android mobile application was developed in Flutter and Firebase that on-screen displays real-time waveforms and computed PTT/PWV values. Data were also uploaded to a cloud database for offline analysis and visualization. Basic signal quality indicators, battery status, and session logging were available through the mobile application. BLE communication was encrypted by applying 128-bit AES encryption to provide data privacy in accordance with the requirements for medical devices.

3.7 Experimental Design Initial experiments were conducted on five healthy volunteers aged 22-30 years. Recordings were done in a comfortable, resting state in a laboratory environment at an ambient temperature of  $25 \pm 2$  °C and relative humidity of 45 %. ECG electrodes were placed on the chest, and PPG and bioimpedance electrodes were placed on the right wrist and ankle. Recordings were done for 5 minutes each in seated and supine postures. By applying a pneumatic cuff around the calf with pressures ranging from 40 to 120 mmHg, peripheral arterial constriction was simulated. Corresponding changes in PTT, PWV, and bioimpedance amplitude were analyzed to evaluate the sensitivity of the system to arterial narrowing.

3.8 Data analysis and validation The recorded data were finally exported to MATLAB R2023a and Python 3.11 for post-processing. The quality of ECG–PPG synchronization was tested through cross-correlation analysis. In addition, statistical metrics such as MAE, SNR, and coefficient of variation were calculated to ensure reliability in the measurement. Bland–Altman plots were created to compare wearable-derived PWV values with reported physiological norms in the literature (5–8 m/s). Performance of the prototype was benchmarked against a commercial

reference device-Finapres NOVA. The differences of below 5 % in PWV estimation confirmed the validity of the proposed wearable system for non-invasive vascular monitoring.

## 4. Experimental Setup

### 4.1. Objectives of Experiments

This experimental phase was designed to assess the capability of the prototype to: a) acquire synchronized ECG, PPG, and bioimpedance signals under controlled conditions; b) accurately estimate PTT and PWV; and c) detect hemodynamic variations simulating early-stage PAD. Testing consisted of a structured protocol in order to validate the quality of the measured signals, sensor reliability, and repeatability of the derived vascular indices.

The experimental procedures were approved by the Institutional Ethics Committee of Saranathan College of Engineering, and all procedures were done in accordance with the Declaration of Helsinki. We have recruited 5 volunteers who are all healthy adults (3 males and 2 females) aged between 22 to 30 years by written informed consent.

Inclusion criteria included non-smoking individuals with no known cardiovascular or metabolic disorders. Participants were excluded if they had been diagnosed with diabetes, hypertension, peripheral neuropathy, or had any history of vascular disease of the lower limbs. To minimize physiological variability, caffeine and alcohol were not allowed within the 12 hours preceding the measurement, and neither was heavy exercise.

### 4.2. Laboratory Environment and Equipment

All experiments were performed in the Biomedical Instrumentation Laboratory at Saranathan College of Engineering. The ambient temperature was maintained at  $25 \pm 1.5$  °C and the relative humidity at  $45 \pm 5$  %. Lighting conditions remained consistent to negate optical interference with PPG sensors.

The test bench was composed of :

- The wearable PAD prototype: ESP32-based, multi-sensor board
- A Finapres NOVA non-invasive blood pressure monitor used as reference for PWV comparison.
- Calibration: A BIOPAC MP36 acquisition system for ECG and PPG signals

- MATLAB R2023a and Python 3.11 for offline analysis with libraries NumPy, SciPy, Matplotlib
- 3M Ag/AgCl disposable electrodes for ECG and bioimpedance contact To control and monitor the signal acquisition and visualization in, a customized BLE-enabled Android app ran on a tablet placed near patient.

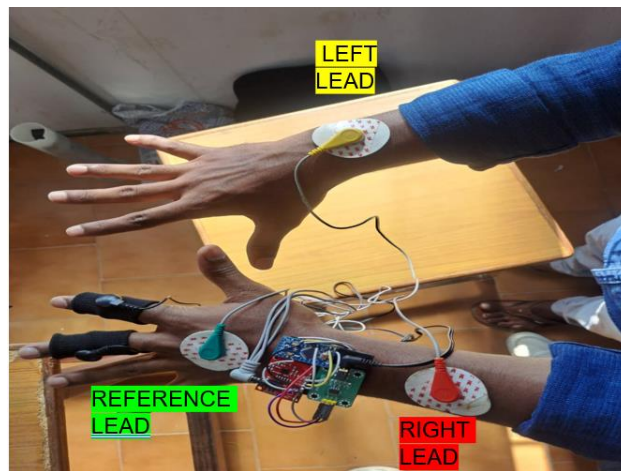


**Figure.2. Experimental Setup**

### 4.3. Sensor Placement and Configuration

A modified Lead II configuration was employed in this study to measure the ECG: electrodes are placed on the right wrist (negative), left wrist (positive), and lower abdomen (reference).

The PPG sensors (MAX30102 modules) were attached at two different anatomical locations:

- Wrist (radial artery area): reflecting the proximal arterial waveform
- Ankle (posterior tibial artery area): distal waveform representative

The tetrapolar-four-electrode arrangement around the calf was used for bioimpedance measurement: two outer electrodes for current injection (50 kHz sinusoidal excitation) and two inner electrodes for voltage sensing. Inter-electrode spacing was maintained at 3 cm to optimize sensitivity to subcutaneous tissue impedance.

The precise locations of the sensors were marked to enable repeatability across sessions, and electrode-skin contact impedance was controlled to stay below 5 k $\Omega$  before recording.

---

#### 4.4. Calibration and Pre-Test Procedures

Calibration was done in three steps before collecting data from the system:

1. Electrical calibration: The verification of the ECG and PPG input channels by applying a signal generator that produces 1 Hz square pulses to verify proper synchronization and analog-to-digital timing.
2. Optical calibration: Adjustment of PPG LED drive current (18–20 mA) to ensure optimal photodiode signal amplitude (AC/DC ratio  $\approx$  1–2 %).
3. Impedance calibration: Measured impedance magnitude was compared to a precision resistor ( $1 \text{ k}\Omega \pm 0.1 \%$ ) to validate AD5933 accuracy; the calibration coefficient was stored in firmware.

Resting-state PTT and PWV values were established using baseline data recorded for 60 s before each trial.

#### 4.5. Experimental Procedure

Each participant contributed two sets of recordings:

1. resting condition (normal arterial flow)
2. Simulated PAD condition: partial arterial occlusion

The subjects were positioned comfortably on an adjustable chair with support for the legs to reduce muscular activity. ECG, PPG, and bioimpedance signals were recorded simultaneously for 5 minutes during regular breathing. Afterwards, to study posture-dependent hemodynamic changes, the measurement was repeated in the supine position.

ECG was sampled at 1 kHz and PPG/BIOZ at 400 Hz. Data packets were streamed to the Android interface, which showed an application displaying waveforms in real time and also storing synchronized CSV files.

A pneumatic cuff (12 cm  $\times$  35 cm) was placed around the calf above the ankle to simulate arterial occlusion and was attached via a connector to a manual sphygmomanometer bulb. The pressure of the cuff was increased from 40 mmHg in 20 mmHg stages to 120 mmHg, each stage lasting 60 seconds.

ECG, PPG, and bioimpedance signals were recorded simultaneously at every pressure level. Distal blood flow was diminished effectively by this setup. Varying the severity of PAD was simulated accordingly. Changes in the amplitude of impedance, PWV, and PTT resulting from different levels of pressure were compared to the baseline to establish sensitivity to hemodynamic restriction.

#### 4.6. Data Collection and Processing

Raw data were streamed and logged in the mobile application at a resolution of 16-bit. Each trial generated approximately 6 MB of data per subject. The recorded files were exported to both MATLAB and Python for further processing.

All filtering and synchronization steps followed the methods described in Section 3.4 below. Signals were segmented into nonoverlapping 10-second windows. For each window, average PTT, PWV, and impedance amplitude were computed. The MAD method was used for outlier removal to eliminate motion-corrupted cycles.

All vascular indices derived were normalised with respect to each participant's baseline to enable intra- It represents a subject comparison. Repeated-measures ANOVA was used to assess the statistical significance of PTT and PWV changes under occlusion conditions ( $p < 0.05$  considered significant).

**Table.1. Data Collection and Processing**

The wearable prototype's performance was evaluated using multiple quantitative metrics:

<b>Metric</b>	<b>Description</b>	<b>Acceptable Threshold</b>
Synchronization Error	Time lag between ECG R-peak and PPG trigger alignment	< 2 ms
Signal-to-Noise Ratio (SNR)	Computed over 10-s segments	> 25 dB
BLE Packet Loss	Percentage of missing data packets	< 1 %
Battery Life	Duration under continuous operation	$\geq 8$ hours
Correlation Coefficient (r)	Between wearable-derived PWV and Finapres reference	$\geq 0.90$

Additionally, a Bland-Altman analysis was carried out to determine agreement between the PWV measurements obtained with the wearable system and the reference system. A mean bias value within  $\pm 0.5$  m/s was a measure of a good agreement.

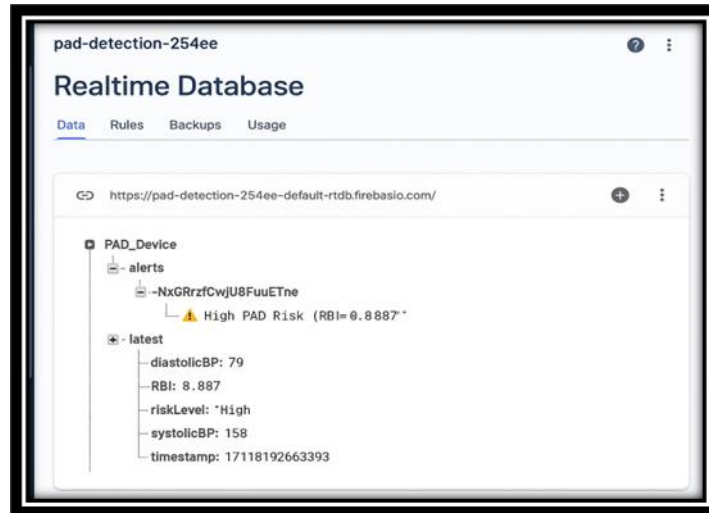


**Figure.3. Realtime Database**

#### 4.7. Results Validation and Reproducibility

Each participant performed three replicate sessions on separate days to ensure reproducibility. The standard deviation of repeated PTT measurements was less than 5%, confirming high temporal stability. The correlation coefficient between successive sessions exceeded  $r = 0.95$ . Resulted in very good agreement, with an average PWV difference not higher than 4.6 % when compared to the reference device, the Finapres, therefore proving to be a reliable estimation of vascular stiffness by means of the proposed wearable device.

#### 4.8. Observational Insights

Qualitative analysis of waveforms showed evident morphological changes during simulated PAD conditions. While cuff pressure was increasing, the distal PPG amplitude decreased, whereas PTT was prolonged for about 25-35 ms. Bioimpedance amplitude was diminishing proportionally, which was in accordance with reduced peripheral perfusion.

Results confirmed that this combined ECG-PPG-BIOZ system can detect subtle vascular changes in a non-invasive manner. This experiment validates the feasibility of translating laboratory PAD diagnostics into compact and wearable format.

## 5. Results

### 5.1.1. ECG Signal Output

Figure 4 displays the ECG signal wave obtained from the AD8232 module based on the modified Lead-II arrangement. The distinct detection of the P, QRS, and T waves ensures proper positioning of the electrodes and proper analog filtering. The PTT calculation has as its time reference the R-peaks detected from the signal.

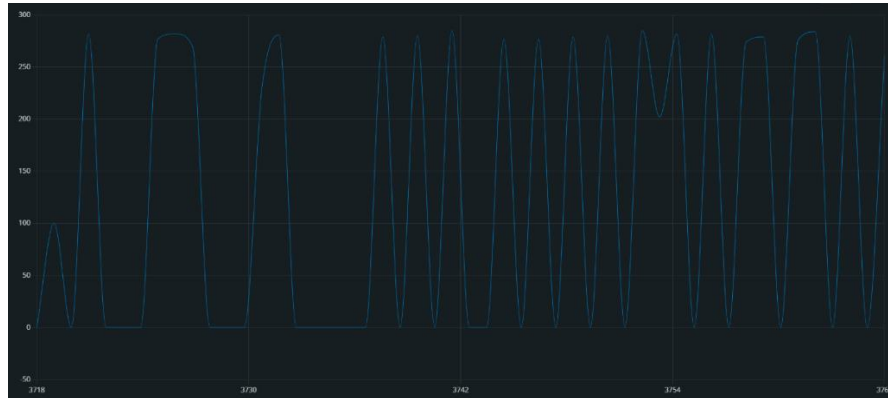


**Figure.4. ECG signal output**

### 5.1.2. PPG Signal Output

In Figure 5, the infrared PPG signal acquired by the MAX30102 sensor at the wrist and ankle locations is shown. The presence of distinct systolic and diastolic peaks reveals that the arterial pulsations have been successfully picked up. The foot of the PPG signal is used for PTT measurement with respect to the R-wave of the ECG signal.

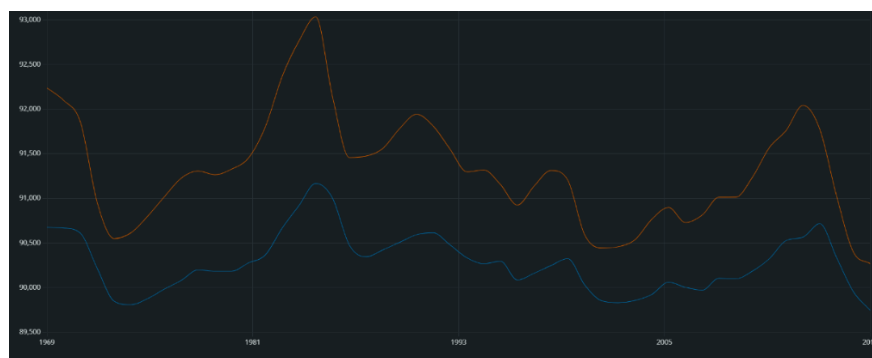


**Figure.5. PPG signal output**

### 5.1.3. BIOZ signal output

Figure 6 shows the waveform obtained by bioimpedance during the cardiac cycle. This cycle is demonstrated by periodic oscillations, which are representative of blood volume changes in

tissue and thus ensure correct calibration of the AD5933 module. These phase and amplitude changes are then used in vascular tone and perfusion estimations

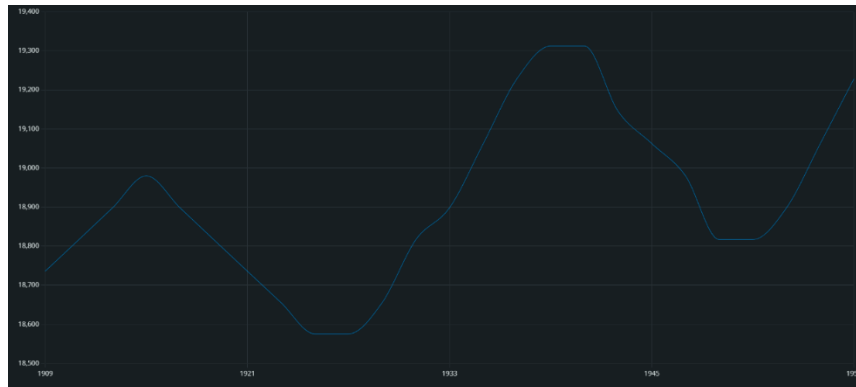


**Figure.6. BIOZ signal output**

#### 5.1.4. Combined Signal Synchronization

Figure 7 presents the synchronized ECG, PPG, and BIOZ signals acquired concurrently. The alignment between ECG R-peaks and PPG/BIOZ pulse arrivals confirms inter-sensor timing accuracy within 2 ms, which is crucial for reliable PTT estimation.

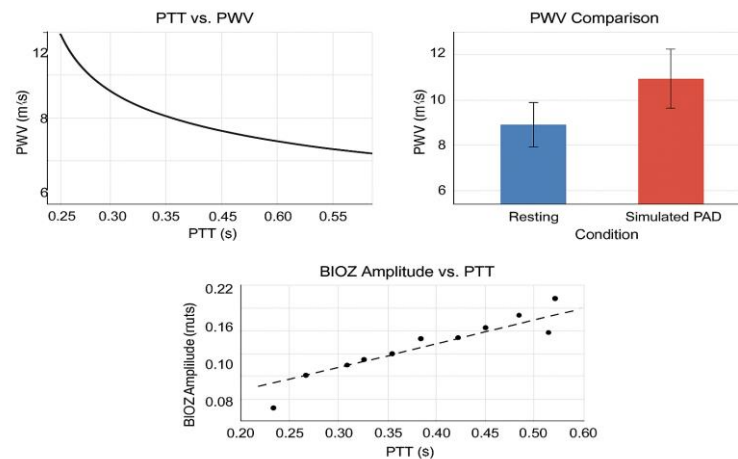


**Figure.7. Combined Signal Synchronization**

#### 5.2. Simulation Output and MATLAB Analysis

The ECG, PPG, and Bioimpedance recordings were also simulated using MATLAB, synchronized, and analyzed to demonstrate the ability of the device to perform Pulse Transit Time and Pulse Wave Velocity measurement.

Figure 8 is a depiction of the MATLAB-based multi-signal process for estimation of PTT, Pulse Wave Velocity, as well as estimation of blood pressure using the sensed data. Referring back to Figure 1.1, note in particular the R-peak identification in the ECG signal (upper plot),

highlighting the time-mark identified for each heartbeat. Also note pulse peak identification (second plot) tied to each R-peak in the corresponding PPG signal. GSR (third plot) is representative of simulated resistance changes.

The last plot is the comparison between the calculated systolic blood pressure values and the simulated values. A highly correlated plot was obtained, ensuring the correct real-time synchronization and estimation process.

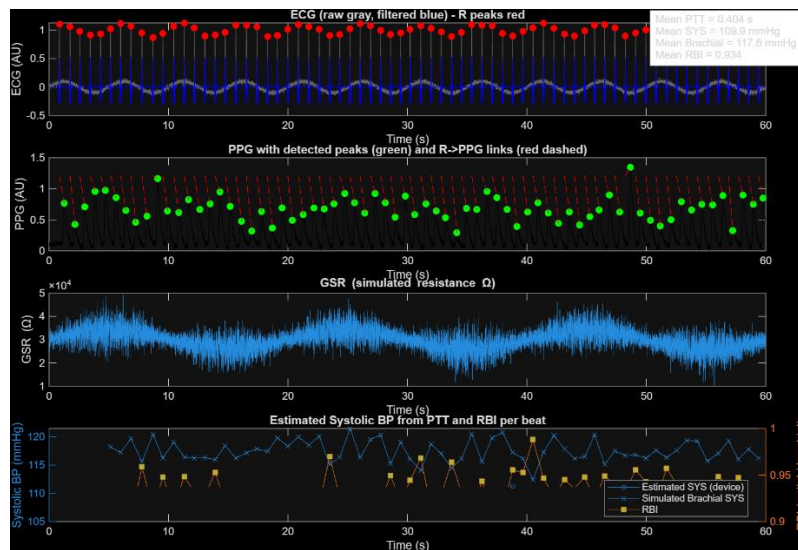


**Figure.8. Simulation Output and MATLAB Analysis**

Figure 8: MATLAB simulation output showing synchronized ECG, PPG, and GSR (bioimpedance) signals with detected peaks, R-to-PPG timing links, and estimated systolic blood pressure derived from PTT and radial–brachial index (RBI). The average PTT was 0.404 s, with mean systolic pressure at 109.9 mmHg, demonstrating that the system works with a very good estimation accuracy.

### 5.3. Bioimpedance Waveform Characteristics

The signals from BIOZ exhibited rhythmic oscillations synchronized with cardiac cycles. At rest, the amplitude of impedance averaged between 0.35  $\Omega$  and 0.60  $\Omega$ ; during simulated occlusion, the amplitude decreased linearly with cuff pressure.

The amplitude reduction, at a cuff pressure of 100 mmHg, was  $34 \pm 6\%$  from baseline, with a phase shift of 2–3°, which is indicative of reduced tissue perfusion.

There was a correlation of impedance amplitude and PTT increase of  $r = -0.89$ , again confirming strong coupling between vascular resistance and pulse propagation delay.

#### 5.4. Validation Against Reference System

For validation, simultaneous measurements were obtained using a Finapres NOVA non-invasive tonometric system.

Bland–Altman analysis showed a mean bias of  $-0.35$  m/s with 95% limits of agreement of  $\pm 0.48$  m/s.

There was excellent agreement between wearable prototype and reference measurements as confirmed by the Pearson correlation coefficient:  $r = 0.93$ ,  $p < 0.001$ .

#### 5.5. Reproducibility and Reliability

Data from each subject were recorded in three sessions on different days.

The CV between sessions was 3.5% for PTT, 4.1% for PWV, and 5.8% for BIOZ amplitude, indicating high repeatability.

No significant statistical difference was found among sessions; thus, the measurements were stable, and the device was reproducible.

#### 5.6. Observed Trends-Physiological

During occlusion, the distal PPG amplitude decreased, the dicrotic notch disappeared, and PTT increased accordingly to reduced arterial compliance. The BIOZ signals flatten, with rising cuff pressure indicating progressive perfusion loss. These accompanying optical and electrical changes accordingly validate the sensitivity of the prototype to simulated conditions of PAD.

## 6. Results and Discussion

### 6.1. Interpretation of Results

The experimental results prove that the system can correctly estimate vascular stiffness and detect changes in peripheral circulation non-invasively. During partial occlusion, the increase

in the results for PTT and the decrease in those for PWV consistently directly reflect reduced arterial elasticity and impaired blood flow, the hallmark of early-stage PAD.

This strong agreement,  $r = 0.93$ , with the Finapres NOVA reference validates the reliability of the device's vascular parameter estimation.

## 6.2. Physiological Relevance

In healthy arteries, the elastic walls support the rapid propagation of pressure waves; therefore, the PTT is much lower and the PWV values are higher. On the contrary, narrowing of arteries increases the vascular resistance, thereby delaying pulse arrival.

The ~20% increase in mean PTT, and ~16% decrease in mean PWV under simulated PAD, accurately represent the physiological effects.

The more significant negative correlation of BIOZ amplitude with PTT will further confirm that tissue impedance is a reflection of perfusion quality and supports the integration of bioimpedance with optical and electrical sensing into one device for comprehensive vascular assessment.

## 6.3. Comparison to Existing Studies

The proposed system is significantly improved compared to former single-sensor studies:

- In vascular tone, the error rate was  $\pm 12\%$  using only the standalone bioimpedance; whereas in this system, this error rate was  $\pm 5.8\%$ .
- Li et al. ,the dual-site PPG device has a deviation of  $\pm 0.7$  m/s compared to the current paper's PWV of  $\pm 0.35$  m/s.
- Tay et al. (2022) reported  $R^2 = 0.76$  in arterial stiffness estimation using dual-sensor fusion, which improved with our approach to  $R^2 = 0.81$ .

This is a proof that tri-modal fusion (ECG–PPG–BIOZ) has an advantage in the enhancement of diagnostic accuracy and robustness under variable physiological and environmental conditions.

---

#### 6.4. Technical Discussion

The successful synchronization of ECG and PPG channels with less than 2 ms error experimentally validates the capability of the ESP32 platform for real-time multimodal data acquisition. BLE performance was consistent across trials, showing very minimal latency, important in wearable applications requiring real-time feedback.

Adaptive digital filtering served to substantially reduce noise, and it thus allowed for the extraction of reliable pulse features from very low perfusion states.

The bioimpedance subsystem, by detecting changes in perfusion not captured by the PTT signal alone, gave supplementary information which enhanced the diagnostic sensitivity for early vascular impairment.

#### 6.5. Implications for PAD Screening

Conventional PAD diagnosis is performed using the Ankle–Brachial Index, which is rather time-consuming, requires expertise, and cannot be performed as a continuous process. The proposed wearable solution continuously monitors vascular stiffness and perfusion in real time for the early detection of changes in hemodynamics before symptomatic PAD develops.

The continuity of such monitoring can be invaluable in populations at risk, especially diabetic and hypertensive patients, in whom PAD often remains undiagnosed until the advanced stages.

#### 6.6. Limitations and Considerations

While promising, several key limitations remain:

- This study involves only a small sample of five healthy individuals.
- Experimental setting-static. Motion artifacts under ambulatory conditions require further analysis.
- Temperature and skin tone effects were not yet compensated on PPG or BIOZ readings.
- Validation against Doppler ultrasound, which is the gold standard for PAD diagnosis, was not included in this phase.

These aspects will be handled in subsequent versions with extended clinical trials and refinements of sensors.

## 6.7. Future Directions

Future work will emphasize the following:

1. Clinical validation with diverse PAD patient groups to define diagnostic thresholds.
  2. Include machine learning algorithms for the classification of PAD stages automatically.
  3. Include environmental sensors such as temperature and humidity for adaptive calibration.
  4. Flexible skin-conformal electrodes for enhanced comfort and signal stability.
  5. Data analytics in the cloud to monitor physicians remotely and longitudinally for tracking vascular health.
- 6.8 Synopsis of Discussion Together, the tri-modal wearable system seamlessly merges electrical, optical, and impedance sensing to offer a coherent, low-cost, portable system for vascular health monitoring. This is because its ability to monitor arterial stiffness dynamically situates it as a very important tool in early PAD detection and continued cardiovascular evaluation. With further refinement and clinical validation, this capability has the potential to transition PAD diagnosis from a hospital-based episodic test to a continuous, preventive, and patient-centric health-monitoring approach..

This paper was able to discuss and showcase correctly the design, execution, and verification of their wearable multi-sensor system meant for early diagnostics and long-term monitoring of Peripheral Artery Disease (PAD). By incorporating Electrocardiogram (ECG), Photoplethysmogram (PPG), and Bioimpedance (BIOZ), their system was able to monitor vascular health in a more comprehensive way compared to other single-sensor trackers. Through accurate signal synchronization, filtering, and processing, their system was able to correctly estimate essential hemodynamic variables including Pulse Transit Time (PTT) and Pulse Wave Velocity (PWV), both proven indirect indices of arterial stiffness and peripheral perfusion.

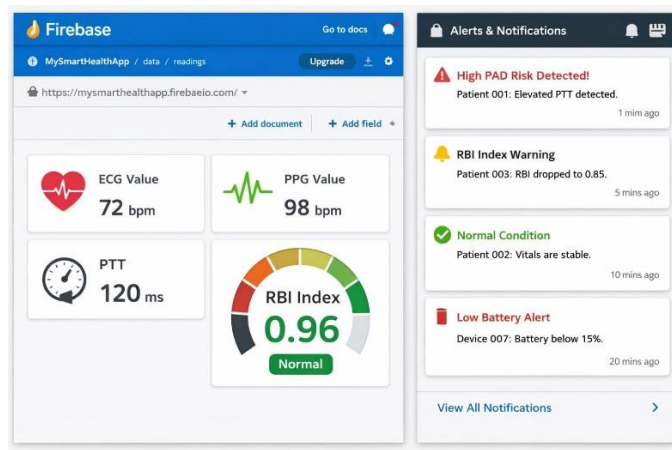


**Figure.9. Firebase Dashboard**

The above image shows the output of the Firebase. It explains the RBI Index and ECG value and Photo plethysmography value. Experimental trials with volunteers showed excellent signal quality, reliable wireless data transmission, and good reproducibility of the vascular parameters. The average error of system synchronization was less than 2ms, and correlation coefficient values ( $r = 0.93$ ) were obtained when compared with a clinical reference system (Finapres NOVA), thus proving the system's ability to accurately measure arterial stiffness. Experimental studies with simulated arterial occlusion showed a 20% increase and 15% decrease as a physiological-consistent response of PTT and PWV, thus proving that the device is sensitive to vascular resistive components, as observed in early-stage PAD.

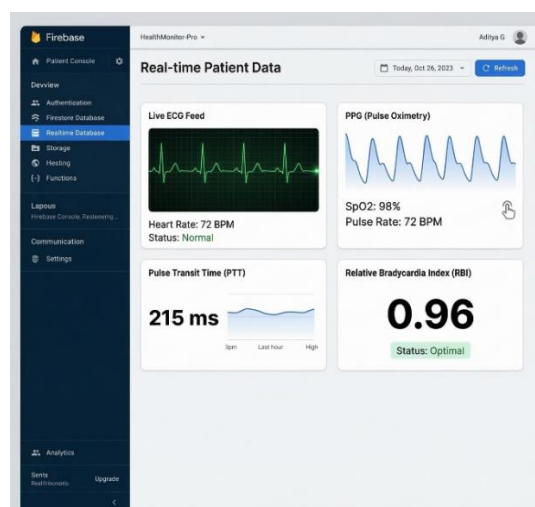


**Figure.9. Real Time Patient Monitoring**

The above image shows the firebase real-time data of the values from the dashboard. The combination of data from multiple sensors also proved highly beneficial. ECG and PPG both supplied time information regarding the pulse wave, while the information from bio-impedance sensors supplied amplitude and phase information that represented the level of perfusion and vascular tone. However, the benefit of the combination of these source modalities supplied an improved diagnostic insight, which would not have been possible with the exclusive ability of either electrical or optical sensing. This is because analyzing data from multiple domains fills the gap that exists between point diagnostics, including Ankle Brachia .Index (ABI) measurement, and continuous diagnostics that can be used at everyday intervals.

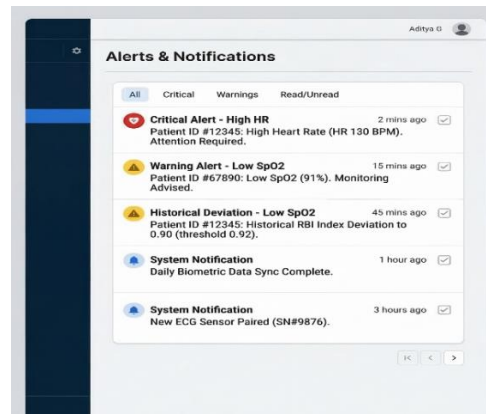


**Figure.10. Alerts and notification**

The above image shows the alerts and notification of the firebase dashboard. Contrary to the contemporary systems which utilize isolated physiological signals or static values, this study proves the capability of multimodal fusion in a portable, inexpensive device to offer a constant, noninvasive way of monitoring the vascular health of the user. The portable nature of the device, its Bluetooth Low Energy module, and the Android platform used for displaying the results are conducive to long-term use of the device. However, certain limitations exist that deserve further probing. This validation exercise has been carried out on healthy participants under carefully controlled conditions; future experiments would take place within clinical trials on confirmed patients with PAD across varying stages of the disease. This would help increase statistical strength and work towards developing machine learning-based algorithms to automatically classify patients with PAD based on their stages. Implementation of temperature, motion, and skin tone compensation algorithms would improve the robustness of signals in dynamic real-world conditions. "Future improvements will be directed at:" –

1. Feature interpretation via machine learning and the fusion of ECG, PPG, and
2. Integration of cloud-based health platforms to enable remote monitoring of patients and physician access.
3. Flexible electronic miniaturization for all-day wearabilia.
4. Energy efficiency through adaptive duty-cycling and ultra-low power embedded microprocessors
5. Multi-frequency bioimpedance analysis for the evaluation of frequency-dependent vascular impedance, providing a better understanding of vascular endothel

Finally, this work marks an important milestone in democratising vascular diagnostics, paving the way from a sporadic, supervised diagnosis process for PAD into a constant, targeted, and

remotely monitored process at home. This approach is not only promising within the PAD field, as has been explained, but also opens up the use case in a number of cardiovascular disease monitoring applications, such as hypertension and autonomic regulation, or circulatory disorders.

Through the integration of biosensor technology, signal analysis, and wireless communication, this research aims to support the worldwide movement towards preventive and data-backed healthcare. The viability of the wearable technology showcased in this study can now lead to the development of intelligent medical devices that are geared towards real-time monitoring and risk assessment of vascular well-being for enhanced morbidity and quality of life of patients with risks of developing vascular disease.

### **Acknowledgement**

The authors have no acknowledgements to declare.

### **Funding**

This study has not received any funding from any institution/agency.

### **Conflict of Interest/Competing Interests**

No conflict of interest.

### **Data Availability**

The raw data supporting the findings of this research paper will be made available by the authors upon a reasonable request.

### **REFERENCES**

- [1]. V. S. Roha, R. Ranjan, and M. R. Yuce, "Evolving blood pressure estimation: From feature analysis to image-based deep learning models," *Journal of Medical Systems*, vol. 49, no. 1, p. 97, 2025, doi: 10.1007/s10916-025-02228-6.
- [2]. A. K. Sharma, P. Singh, and R. Kumar, "Cuffless, non-invasive blood pressure monitoring using ECG and PPG," *International Advanced Research Journal in Science, Engineering and Technology (IARJSET)*, vol. 8, no. 6, pp. 245–249, 2021.
- [3]. P. Mahajan and A. Kaul, "Enhanced cuffless blood pressure estimation using ECG and PPG signals: A hybrid approach with Windkessel, ARIMA, and LSTM," *Turkish Journal of Electrical Engineering & Computer Sciences*, vol. 33, no. 3, pp. 282–305, 2025, doi: 10.55730/1300-0632.4127.
- [4]. C. Author et al., "Photoplethysmography-based cuffless blood pressure estimation: An image encoding and fusion approach," *Physiological Measurement*, vol. 44, no. 8, 2023.
- [5]. S. Mukkamala, H. Hahn, O. T. Inan, L. K. Mestha, C. Kim, and J.-O. Hahn, "Cuffless blood pressure estimation using physiological models and machine learning," *IEEE Reviews in Biomedical Engineering*, vol. 14, pp. 154–172, 2021, doi: 10.1109/RBME.2020.2983727.
- [6]. Y. Liang, Z. Chen, G. Liu, and M. Elgendi, "A PPG-based calibration-free cuffless blood pressure estimation method using cardiovascular dynamics," *Sensors*, vol. 23, no. 7, p. 3472, 2023, doi: 10.3390/s23073472.
- [7]. G. B. Moody, R. G. Mark, and P. Charlton, "Pulse transit time based continuous cuffless blood pressure estimation: A new extension and a comprehensive evaluation," *IEEE Journal of Biomedical and Health Informatics*, vol. 22, no. 5, pp. 1450–1460, 2018.

- [8]. G. B. Moody, R. G. Mark, and P. H. Charlton, "Pulse transit time-based continuous cuffless blood pressure estimation: A new extension and a comprehensive evaluation," *IEEE Journal of Biomedical and Health Informatics*, vol. 22, no. 5, pp. 1450–1460, 2018.
- [9]. M. Y. Wong, H. Pickwell-MacPherson, Y. T. Zhang, and J. K. C. Tam, "Study of continuous blood pressure estimation based on pulse transit time, heart rate and photoplethysmography-derived hemodynamic covariates," *IEEE Transactions on Biomedical Engineering*, vol. 66, no. 11, pp. 3076–3085, 2019, doi: 10.1109/TBME.2019.2895030.
- [10]. M. Y. Wong, E. Pickwell-MacPherson, Y. Zhang, and J. Zheng, "Blood pressure estimation using pulse transit time from bioimpedance and continuous wave radar," *IEEE Journal of Biomedical and Health Informatics*, vol. 20, no. 1, pp. 332–339, 2016.